

# Titanium Dioxide Coated Graphene Nanosheets as a Reinforcement in Aluminum Matrix Composites Based on Pressure Sintering Process

Zheng-Hua Guo (✉ [guo.zheng.hua@163.com](mailto:guo.zheng.hua@163.com))

Nanchang Hangkong University

Qingjie Wu (✉ [wu856200@163.com](mailto:wu856200@163.com))

Nanchang Hangkong University <https://orcid.org/0000-0003-3845-3622>

Ning Li

Nanchang Hangkong University

Li-Hong Jiang

Nanchang Hangkong University

Wen He

Nanchang Hangkong University

Guo-Hui Tan

Jiangxi Jiangling Special Vehicle Co., Ltd.

---

## Original Article

**Keywords:** Graphene nanoplatelets; Titanium oxide coating; 7075Al Alloy; Metal

**Posted Date:** April 28th, 2020

**DOI:** <https://doi.org/10.21203/rs.3.rs-22826/v1>

**License:** © ⓘ This work is licensed under a Creative Commons Attribution 4.0 International License.

[Read Full License](#)

---

# **Titanium Dioxide Coated Graphene Nanosheets as a Reinforcement in Aluminum Matrix Composites Based on Pressure Sintering Process**

Zheng-Hua Guo<sup>\*</sup>, Qing-Jie Wu<sup>\*</sup>, Ning Li, Li-Hong Jiang, Wen He, Guo-Hui Tan

## **Abstract**

Graphene nanoplatelets (GNPs) reinforced 7075 aluminum (Al) nanocomposites were successfully synthesized using the powder metallurgy method. A novel method for optimizing interfacial bonding by coating titanium dioxide (TiO<sub>2</sub>) on the surface of GNPs was proposed in this manuscript. The effects of GNPs on mechanical properties and microstructure of the aluminum matrix nanocomposites, both with and without TiO<sub>2</sub> coating layers, have been investigated. Experimental results showed that the corresponding mechanical properties of the nanocomposites were further improved when the GNPs have TiO<sub>2</sub> coating layers, compared with the addition of pure GNPs. The yield strength, ultimate tensile strength, and microhardness of the nanocomposites reinforced with TiO<sub>2</sub>-coated GNPs increased by 22.9%, 25.9%, and 20.1%, respectively, in comparison to those of the matrix. The further improvement of the mechanical properties could be attributed to the existence of the coating layer, which optimizes the interface bonding between the reinforcement and the matrix, thereby improving the effectiveness of load transfer.

**Keywords:** Graphene nanoplatelets; Titanium oxide coating; 7075Al Alloy; Metal

---

<sup>\*</sup> \*corresponding authors.

E-mail address: [guo.zheng.hua@163.com](mailto:guo.zheng.hua@163.com) (Zhen-hua Guo). School of Aeronautic Manufacturing Engineering, Nanchang Hangkong University, Nanchang, Jiangxi 330063, China.

E-mail address: [wu856200@163.com](mailto:wu856200@163.com) (Qing-Jie Wu). School of Aeronautic Manufacturing Engineering, Nanchang Hangkong University, Nanchang, Jiangxi 330063, China.

matrix composite.

## **1. Introduction**

Graphene, a two-dimensional material consisting six rings of  $sp^2$ -hybridized carbon atoms, has been used as an important new nanosize reinforcement in the field of structural and functional composites since it was successfully separated in 2004<sup>[1-4]</sup>. It has attracted much attention due to the extremely high mechanical strength and excellent thermal and electrical properties. Compared with carbon nanotubes (CNTs), graphene has a larger surface area and lower production costs. The sheet structure of graphene makes it easier to disperse in the matrix, which makes it an excellent alternative reinforcement for composites. Currently, Graphene has been extensively studied to enhance the mechanical and other properties of polymer or metal based composites [5, 6].

Aluminum and aluminum-based composites are widely used in automotive and aerospace enterprises due to low weight and high corrosion resistance. With the development of industry, composites based on aluminum alloy are expected to demonstrate higher mechanical properties. Therefore, more and more materials scientists are trying to reinforce aluminum alloys with a strong, rigid, and lightweight phase [7]. Recently, various efforts have been made on graphene as a reinforcement of aluminum-based composites. Gang Li et al. [8] successfully fabricated a graphene nanosheets (GNSs) /Al nanocomposites by ball milling and vacuum hot pressing. The report showed that the ultimate tensile strength and yield strength of the pure Al could be improved by 56.19% and 38.27% due to the addition of GNSs. The microhardness

of the nanocomposites improved significantly as the content of GNSs increased. Haiping Zhang et al. [9] reports the similar results by adding 1wt. % GNPs to Al5083 alloy. They revealed that a high strengthening efficiency of the multi-layer GNPs may be mainly attributed to shear lag (load transfer) effect and grain refinement. And the nanosized Al<sub>4</sub>C<sub>3</sub> formed could also act as a reinforcement. Moreover, the composite successfully prepared by Jingyue Wang et al. [10] exhibited a tensile strength improvement of 62% increment over unreinforced matrix with only 0.3 wt. % GNSs addition. However, despite some progress in the field of nanocarbon-reinforced aluminum-based composites, there are still some important issues remain to be resolved. The main problem is insufficient interface bonding between the nano-carbon material and the aluminum alloy, which results in that stress cannot be completely transferred from the matrix to the reinforcement during loading [11].

In order to optimize the wettability and interfacial bonding between nano-carbon materials and alloy matrix and further improve the final mechanical properties of the corresponding composite, surface modification techniques have been adopted in the field of nano-carbon reinforcement by materials scientists. CNTs coated SiC nano-layer were prepared by Yongha Park et al. [12] using solid heating reaction method between silicon powders and CNTs ( $C + Si \xrightarrow{1573K} SiC$ ). The report exhibited that the CNTs with SiC coating layer resulted in an improvement of the wettability and bonding strength in Mg-based composite. Carbon nanofibers (CNFs) coated with copper were also used to enhance the mechanical properties of magnesium alloys [13]. The result indicated that the enhanced of wettability between Al and CNFs as well as

the free of Al<sub>4</sub>C<sub>3</sub> are related to the Cu coating layer. There are a lot of reports about carbon nanotubes being coated with metal or nano-ceramic particles as a reinforcement to strengthen the properties of metal matrix composites, which reflect the beneficial effect of the coating on interfacial bonding and mechanical properties. However, so far, the investigations on Al composites reinforced with coated graphene are still limited.

In this study, based on the 7075 aluminum alloy, the nanocomposites reinforced with TiO<sub>2</sub> coated graphene nanoplatelets (TiO<sub>2</sub>@GNPs) and purified GNPs were prepared by means of Pressure Sintering. The effects of the TiO<sub>2</sub>@GNPs and the purified GNPs on the microstructure and the mechanical properties of the nanocomposites fabricated were characterized and investigated. Furthermore, the mechanisms for enhancing the mechanical properties of nanocomposites were also discussed in detail.

## **2 Experimental procedures**

### **2.1 Materials**

Commercial 7075 aluminum alloy powders (purity 99.7%, particle size 70~120 μm, from Shenyang Nonferrous Metal Research Institute, China) were used as the matrix material for this study. Table 1 shows the chemical composition of the aluminum powder. The starting reinforcement, Graphene nanoplatelets (provided by Nanchang Taiyang Nanocrystal Co., Ltd.) have a purity of 98.6 wt. %, an average thickness of 6–8 nm and a particle size of 12~15 μm, respectively.

Table.1 Chemical compositions of 7075Al powder

Type	Zn	Mg	Cu	Fe	Si	Al
Wt pct	5.1~6.1	2.1~2.9	1.2~2.0	0.5	0.4	Bal.

## 2.2 Experimental procedures

The acid-treated 0.2g of GNPs were first placed in 20ml ethanol and sonicated for 10 minutes (90W). 0.5 mL of Tetrabutyl titanate (TBT) and 10 mL of glycerol were added to the resulting solution and sonicated for 5 minutes again. The mixed solution was subsequently transferred to an autoclave and kept in muffle furnace at 160~200 °C for 12 hours. After that, the obtained solution was centrifuged to obtain powder precipitates and then the precipitates were washed with pure ethanol (99.7pct purity) dried at 70 °C for 24hours. The resulting powders were then calcined in argon at 460 ~ 480 ° C for 3 hours. Scanning electron microscopy and transmission electron microscopy were used to study the microstructure of the TiO<sub>2</sub> coated GNPs (TiO<sub>2</sub>@GNPs) after this coating process.

Figure 1 illustrates the synthesis procedure of TiO<sub>2</sub> coated GNPs-7075Al composites. As shown in the figure, 0.5 wt. % of TiO<sub>2</sub>@GNPs and 99.5 wt. % of 7075Al powder were put into corundum mixing tanks containing corundum grinding balls with diameters of 5~20 mm. The initial ball powder weight ratio was 10: 1. The mixing tanks were stirred using a planetary ball mill at 380 rpm for 24 hours in an argon atmosphere. 1 wt. % stearic acid needs to be added as a process control agent to prevent excessive sticking and aggregation of the powders (cold welding) during ball milling. After that, the as-prepared nanocomposite powders were placed in a high-temperature graphite die and subjected to hot-press sintering at 595 °C for 2h in a vacuum of 10<sup>-3</sup> torr under a uniaxial pressure of 28 MPa. The sintering parameters

are shown in Figure 1. For comparison, the alloy without GNPs was also fabricated by the same process.

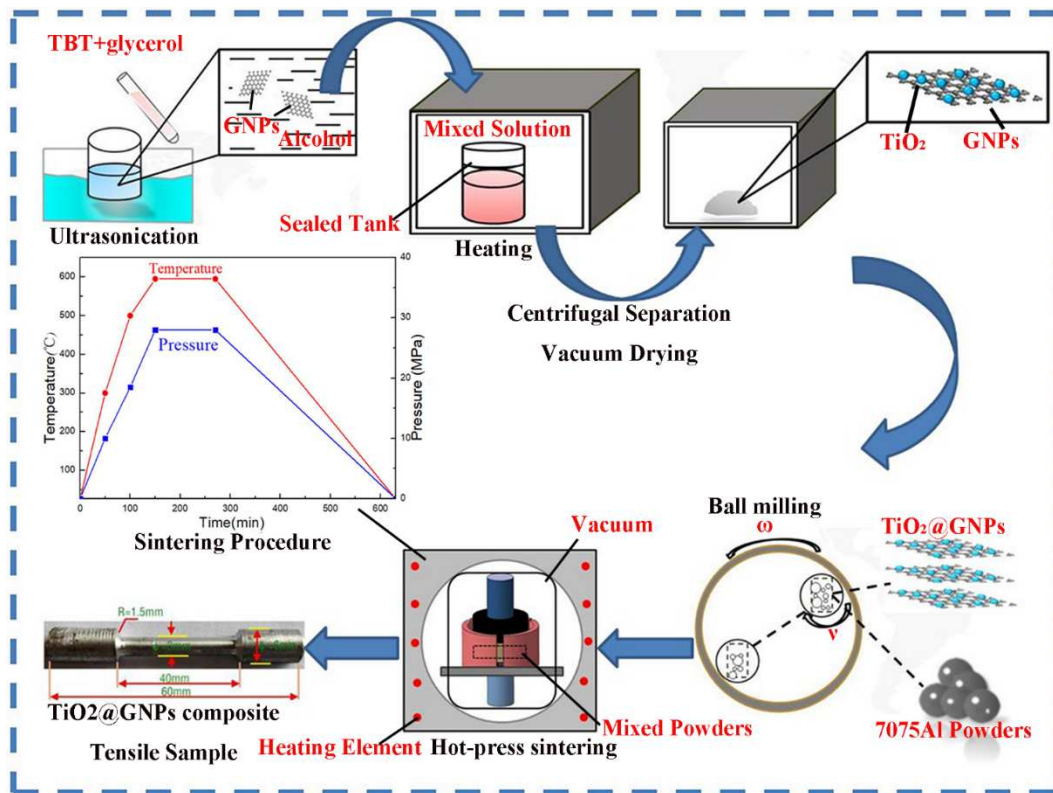


**Figure 1** Schematic of the preparation of TiO<sub>2</sub>@GNPs / 7075Al nanocomposites.

### 2.3 Characterization

Nikon Eclipse MA200 Optical microscope (OM) and NOVA NanoSEM 450 scanning electron microscope (SEM) were used to characterize the microstructures and the fracture surfaces of the GNPs/7075Al nanocomposites. The nanostructures and interfaces of GNPs/7075Al were also investigated using a transmission electron microscope (TEM, JEM-2100). Dimension of specimens for TEM observation is approximately  $\phi$ 3mm and a thickness of 30 $\mu$ m, which prepared by traditional jet-polishing process. Tensile tests were performed on a universal testing machine at ambient temperature using a displacement rate of 0.2 mm/min to investigate the strengthening effect. Microscopic Vickers hardness tester (HVS 1000A) was used to

obtain microhardness values according to standard EN-ISO 14577:2003. The microhardness should be measured at least five times to obtain the average value on each sample.

### **3. Results and discussion**

#### **3.1 Microstructure**

Microstructure of the purified GNPs has been shown in figure 2(a). Correspondingly, figure 2(b) and 2(d) exhibits the typical SEM and TEM images of the coated-GNPs after the coating reaction. It's evident that the surface of most GNPs has been completely covered by a layer of needle-like particles after functionalization. As seen in the TEM image (figure 2(d)), these generated white particles appear to protrude outwards disorderedly from the GNPs surfaces. The corresponding EDX spectrum indicated that the coating layer mainly consists of Ti and O. The relative concentration ratio between Ti and O was approximately 1:2. Meanwhile, it could be noticed that the high resolution TEM (HRTEM) and SAED pattern images show the d-spacings of the nanoparticles are 0.35 nm and 0.2894nm, corresponding to the (1 0 1) (figure 2(e))<sup>[14]</sup>, and (1 0 3(-))TiO<sub>2</sub> planes (figure 2(f)), respectively. Therefore, it could be confirmed that titanium oxide has been successfully generated and coated on the surface of GNPs. In addition, it was observed that TiO<sub>2</sub> nanoparticles did not fall off the surface of GNPs even after sonication during TEM sample preparation. This phenomenon indicates that a strong interfacial bond has been formed between nanoparticles and GNPs <sup>[15]</sup>.

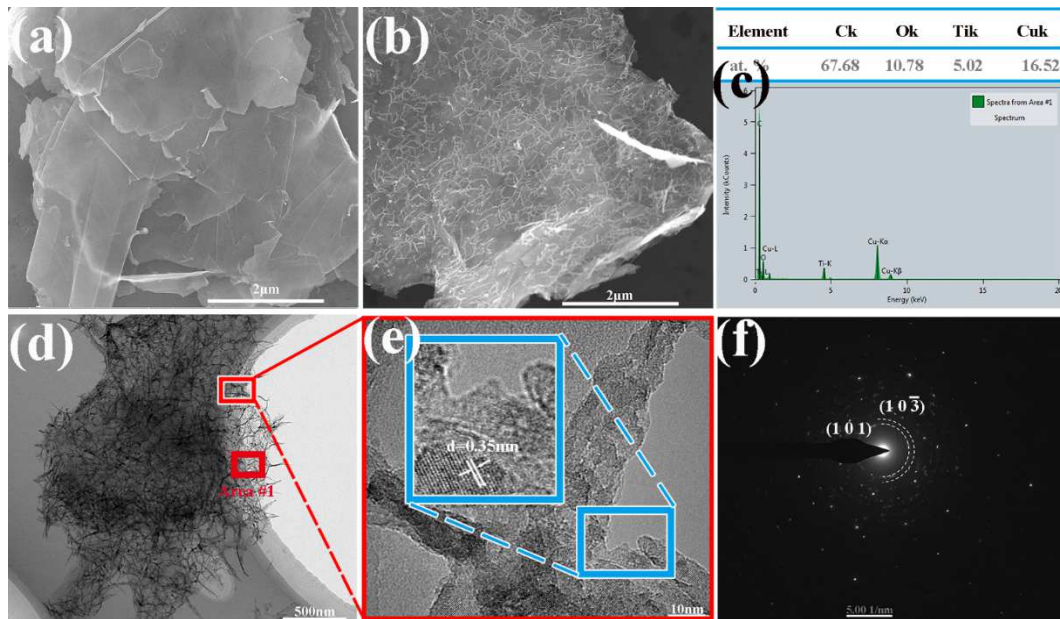


**Figure 2** SEM and TEM images of  $\text{TiO}_2@\text{GNPs}$ : (a) SEM image of GNPs. (b) SEM image of  $\text{TiO}_2@\text{GNPs}$ . (c) EDX results of Area#1. (d) TEM image of  $\text{TiO}_2@\text{GNPs}$ . (e) HRTEM image of  $\text{TiO}_2@\text{GNPs}$ . (f) SAED patterns of  $\text{TiO}_2$  layer.

Figure 3 shows the irregularly shaped, raw 7075Al particles with the size of approximately 70~120 nm in diameter. After milling, the morphologies of the 7075Al-0.9 wt. % GNPs powders were more spherical with a rounded flattening tendency than that those of the raw 7075Al particles as shown in figure 3(b). The size of the particles was also significantly smaller. Meanwhile, it can also be seen from figure 3(c) that some individual GNPs (labeled with arrows) with  $\text{TiO}_2$  are embedded in the particles. It suggests that GNPs with  $\text{TiO}_2$  are uniformly dispersed in the surface of 7075Al particles or trapped in soft matrix by the ball milling process. In general, 7075Al powders are easily broken into small particles due to the shearing force by ball milling. The milling process could cause these composite particles to collide between the inner surface of the containers and the balls and generate enough energy to change the shape of the powders. Eventually, the particles are crushed and flatted at

the end of the milling [16]. The GNPs then be incorporated into the Al powers through plastic deformation during the milling process.

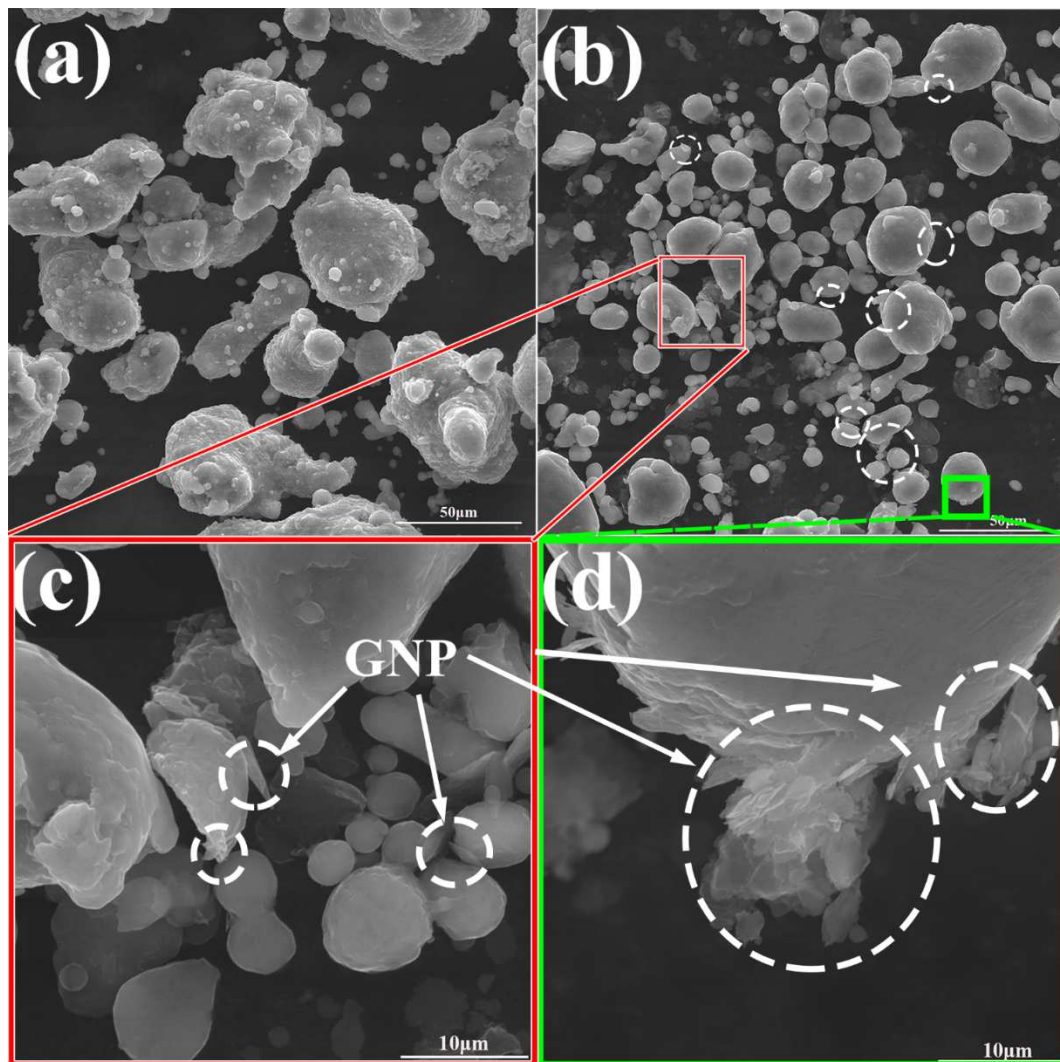


**Figure 3** Micrographs of composite precursor powders

The SEM images of the matrix alloy and GNPs/7075Al nanocomposites are shown in the figure 4. It can be seen from figure 4(b) and (c) that the grain size of the alloy matrix becomes smaller after adding GNPs or  $\text{TiO}_2\text{@GNPs}$ . This phenomenon indicated that the GNPs addition had an effect of refining the matrix grains due to the fact that GNPs distributed at the grain boundaries could hinder the grain growth [9]. In addition, some micropores were revealed on the surface of the alloy and

GNPs/7075Al samples, presumably due to the uneven grain refinement in the matrix. It can also be seen from figure 4(b) that agglomerations of GNPs appeared at the grain boundaries. It could be attributed to the poor dispersibility and wettability of the GNPs in the matrix [17]. As shown in figure 4 (c), no obvious reinforcement agglomeration occurred at the grain boundaries of the composite with added TiO<sub>2</sub>@GNPs. This phenomenon is mainly results from the optimization of the wettability of GNPs with the matrix and thus promotes the combination of GNPs and alloy, which leads to a reduction in structural defects during the process.

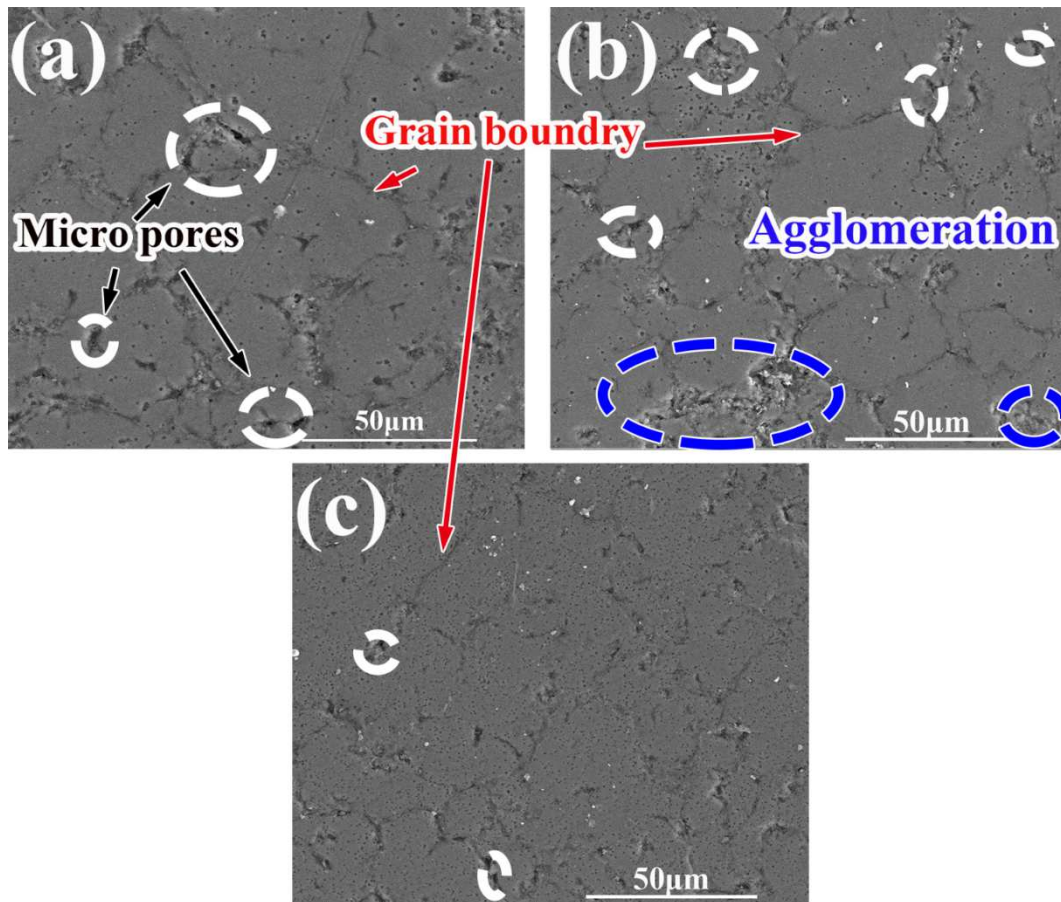


**Figure 4** Micrographs of 7075Al and corresponding nanocomposites: (a) 7075Al, (b) GNPs/7075Al, (c) TiO<sub>2</sub>@GNPs/7075Al

Figure 5 displays the interface structure of 7075Al nanocomposite containing

TiO<sub>2</sub>@GNPs. As shown in figure 5(a), the carbon plane-structure was clearly visible and parallel to the matrix, which indicated that the GNPs maintains its multilayer structure after the preparation process at 595 °C. Moreover, the interface between GNPs and matrix was tightly attached in the nanocomposite without obvious gaps or impurities, suggesting a sound interface between the GNP and the Al matrix [18]. In addition, it can be observed from the HRTEM images (figure 5 (b) and (c)) that there are some needle-like or sphere nanoparticles on the surface of GNPs. The d-spacing of these nanoparticles provided by SAED pattern (Fig. 5(d)) were 0.2319 nm, 0.2133 nm, and 0.1370 nm, corresponding to the (22(-) 2(-)), (13(-)2) and (322(-)) planes of TiO<sub>2</sub>. Therefore, it can be confirmed that the TiO<sub>2</sub> nanoparticles were still present and in close contact with the GNPs surface.

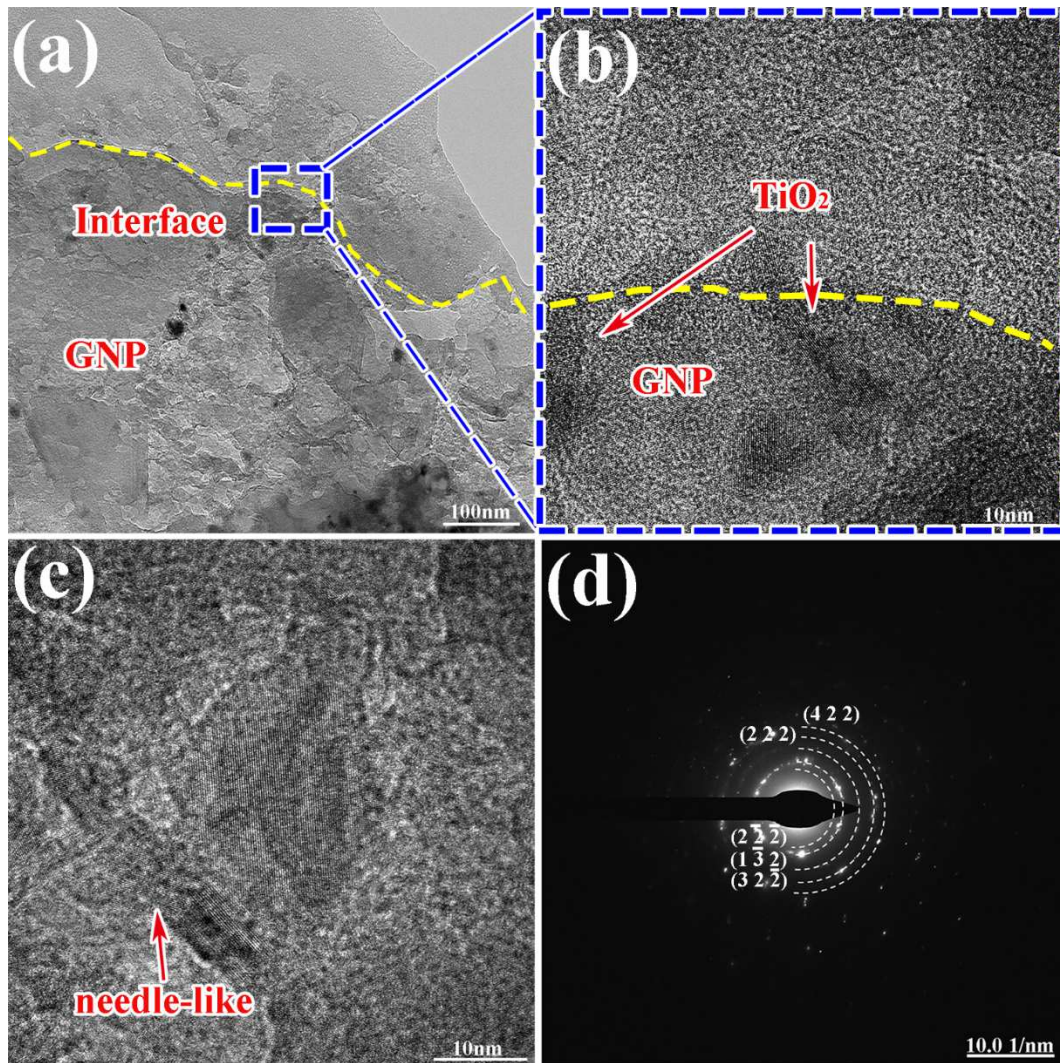
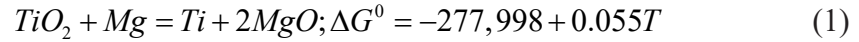


**Figure 5** TEM images of (a), (b) and (c)  $\text{TiO}_2$ @GNPs/7075Al nanocomposites fabricated, (d) SAED patterns of coating layer.

It is worth noting that magnesium oxide (MgO) nanoparticles appeared near the coating layer according to the results of figure 5(d). In other words, a few MgO nanoparticles were formed and embedded at the interface except for  $\text{TiO}_2$  nanoparticles. The d-spacing measurements of MgO are 0.1196 nm and 0.0889nm, corresponding to the (222) and (422) planes [15]. The generation of MgO could be attributed to a chemical reaction between GNPs and  $\text{TiO}_2$  nanoparticles. The interfacial reaction can be described [19] as in Eq. (1):



When the free energy calculated is lower than zero, the reaction proceed in according to the Eq. (1). Hereinafter, the highest sintering temperature provided by the equipment in the current process is 595 ° C (868K). The calculation results showed that the free energy of reaction is less than zero. It implied the possibility of this reaction.

### 3.2 Mechanical Properties

The mechanical properties of 7075Al and the nanocomposites reinforced by purified GNPs or TiO<sub>2</sub>@GNPs are given in figure 6. As shown in figure 6(a), the yield strength (YS) and ultimate tensile strength (UTS) were improved due to the addition of the reinforcements. Notably, the addition of reinforcement TiO<sub>2</sub>@GNPs instead of purified GNPs further promoted the improvement of the mechanical properties. In the case of the GNPs/7075Al nanocomposite fabricated, the YS and UTS was 232 MPa and 310 MPa. On the other hand, the YS and UTS of the nanocomposite reinforced with TiO<sub>2</sub>@GNPs were 258MPa and 340MPa, increasing by 22.9% and 25.9%, as compared to the matrix. Furthermore, the addition of GNPs with/without TiO<sub>2</sub> coating layer into 7075Al alloy leads to an increase of microhardness of the GNPs/7075Al nanocomposites. The microhardness values of GNPs/7075Al and TiO<sub>2</sub>@GNPs/7075Al remarkably increased to 109.4HV and 116.2HV respectively, as compared with the matrix (96.7 HV). The further enhancement of the tensile properties and microhardness of these prepared nanocomposites could be attributed to the optimized interfacial bonding due to the

presence of the TiO<sub>2</sub> coating layer [19, 20].

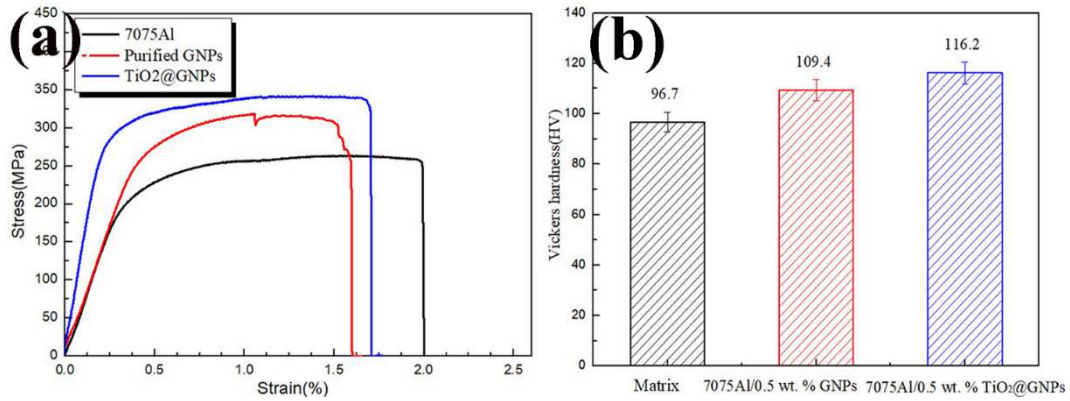


**Figure 6** Mechanical behaviors of 7075Al matrix and its nanocomposites reinforced with purified GNPs or TiO<sub>2</sub>@GNPs

Strengthening mechanisms of elongation refining, dislocation strengthening and stress transfer are commonly used to explain the improvement in mechanical properties, especially yield strength of GNPs/Al composites. In general, the existence of a huge difference between the coefficient of thermal expansion (CTE) of GNPs ( $0.9 \times 10^{-6} \text{K}^{-1}$ ) and Al alloy ( $2.36 \times 10^{-5} \text{K}^{-1}$ ), which led to the occurrence of prismatic punching at the interface, and then resulting in the strengthening of the nanocomposites. Increase in YS of nanocomposites due to this mechanism [21] can be calculated by following Eq. (2):

$$\sigma_{CET} = 1.25Gb \sqrt{\frac{12\Delta T \Delta C f_v}{bd_p}} \quad (2)$$

In the Eq. (2),  $G$  is the shear modulus of Al ( $0.26 \times 10^5 \text{ MPa}$ ),  $\Delta T$  is the change in temperature,  $\Delta C$  is defined as the CET difference between GNPs and the matrix.  $f_v$  and  $d_p$  are the volume fraction and average diameter of GNPs, respectively.  $b$  is burger vector of matrix (0.286 nm).

On the other hand, the addition of purified GNPs or TiO<sub>2</sub>@GNPs resulted in a

refinement of the matrix alloy. Accordingly, the increase in YS can be calculated by Hall–Petch equation :

$$\Delta\sigma_{Hall-petch} = K(d_{com}^{1/2} - d_{matrix}^{1/2}) \quad (3)$$

The  $d_{com}$  and  $d_{matrix}$  are the average grain size of the composite fabricated and the alloy. K denoted the H-P coefficient of the matrix alloy (0.04 MPa for Al). As can be seen from the figure 4, the nanocomposites fabricated showed only a slight tendency of grain refinement after the addition of GNPs. Compared with other strengthening mechanisms, the grains refinement has a very small proportion of the improvement effect of composites strength [15]. Therefore, the strengthening of nanocomposites by grain refinement was ignored in this manuscript.

Furthermore, the most important strengthening mechanism model among the three strengthening mechanisms is the shear lag model, which explains the load transfer from the matrix to the reinforcement. In short, the applied load can be transferred from the matrix to the reinforcement at the interfacial shear stress.

Increase in YS of composites can be calculated by Kelly-Tyson model [22] as follows:

$$\Delta\sigma_{LT} = \frac{f_v}{2} \sigma_m \quad (4)$$

In Eq. (3),  $f_v$  represents the volume fraction in also.  $\sigma_m$  is the YS of the matrix.

According to the calculation results of Eq. (2) and (4),  $\Delta\sigma_{CET}$  and  $\Delta\sigma_{LT}$  are 55MPa and 84MPa, respectively. The theoretical predictions are much larger than the experimental data of YS. There are two possible reasons for this difference. First, load transfer prediction is based on that all GNPs in alloys are perpendicular to the

stretching direction. However, in fact, the location and orientation of GNPs in the matrix are random [21]. Second, the theoretical prediction of YS is based on the assumption that all the added GNPs are evenly dispersed in the matrix. These simple assumptions reduce the prediction accuracy of the effective contribution to yield strength [23].

In addition, stress transfer is considered to be a critical enhancement mechanism as mentioned before. It provides the greatest contribution to nanocomposite strengthening. Therefore, the strong bonding interface and the wettability directly affect the final properties of the GNPs reinforced Al-based nanocomposites fabricated. In the case of the GNPs/7075Al composite, GNPs aggregation occurred at the grain boundaries during the preparation process due to the poor wettability and interfacial adhesion of GNPs as shown in the figure 4. It weakens the strengthening effect of GNPs on the mechanical properties of the nanocomposite. On the other hand, the existence of the TiO<sub>2</sub> coating layer improves the interface bonding between the reinforcement and Al matrix. Meanwhile, the products generated on the coating are believed to lead to an enhanced anchoring effect by the Al alloy matrix. These facilitate efficient transfer of loads from the matrix to the GNPs [20]. Hence, the mechanical properties of Al-based nanocomposites reinforced with TiO<sub>2</sub>@GNPs are better than those of nanocomposites with uncoated GNPs.

The representative fracture surface characterization of 7075Al and the nanocomposites fabricated have been shown in figure 7. Correspondingly, the results of EDS analysis has been shown in the figure 7(f). The fracture surface of the matrix

exhibits the mixed fracture and characterized by the significant dimples and platforms (figure 7(b)). In nanocomposites prepared reinforced with GNPs (figure 7(b)), some pullout of GNPs was observed and the number of the platforms has decreased. However, two large cracks were visible on the fracture surface. These cracks show a propagating and growing trend under the bending load. When the reinforcement has been replaced by  $\text{TiO}_2@\text{GNPs}$ , the fracture surfaces of the sample exhibit few cracks, while the significant pull-out of GNPs, indicating the interfacial bonding between GNPs and 7075Al has been improved due to the coating layer. EDS result revealed that these phases were composed by the major elements of Al, C, O, Mg and Ti, confirming that the phases were GNPs and  $\text{TiO}_2$ .

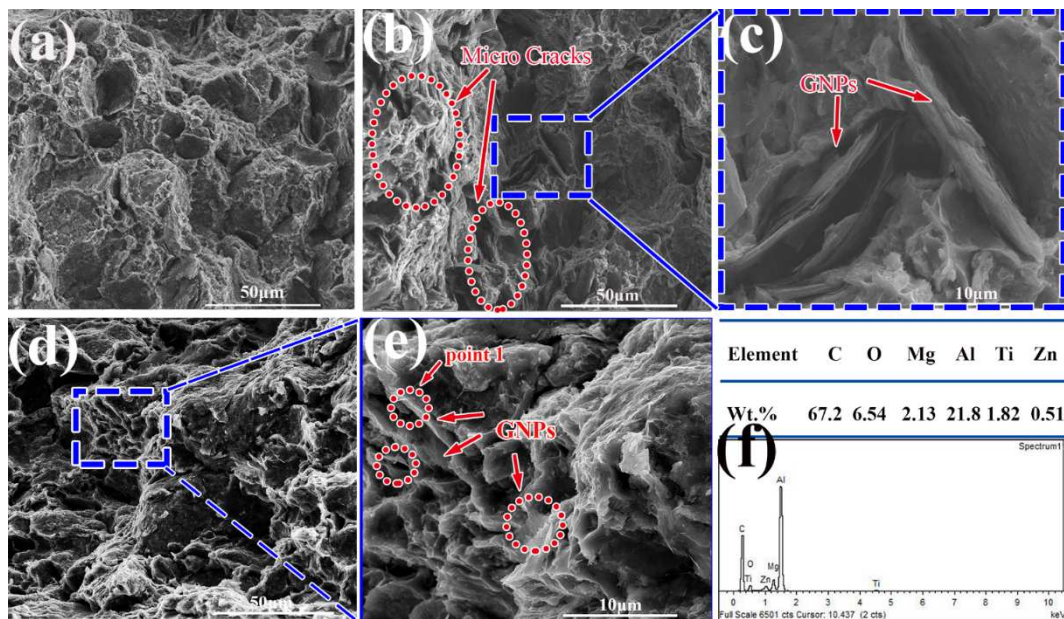


**Figure 7** SEM fractographs of composites with GNPs or  $\text{TiO}_2@\text{GNPs}$ : (a)7075 matrix (b-c)with GNPs (d-e)with  $\text{TiO}_2@\text{GNPs}$  (f)The EDS results of point 1.

#### 4 Conclusions

7075Al composites reinforced with  $\text{TiO}_2@\text{GNPs}$  were successfully fabricated by hot-press sintering combined with ball-milling in the current study. The addition of

TiO<sub>2</sub>@GNPs to Al-based nanocomposites can effectively reduce the probability of reinforcement agglomeration at the grain boundaries compared to the nanocomposites reinforced by purified GNPs. Additionally, the mechanical performances and Vickers hardness of the nanocomposites were further improved when the GNPs have TiO<sub>2</sub> coating layers, compared with the addition of pure GNPs. The YS, UTS and microhardness of the TiO<sub>2</sub>@GNPs/7075 Al nanocomposite fabricated were 22.9%, 25.9%, and 20.1% higher than those of the matrix alloy, respectively. The improvement in mechanical properties can be attributed to grain refinement, coefficient of thermal expansion and load transfer mechanism. Among them, the load transfer is believed to provide the maximum contribution to composite strengthening. The existence of TiO<sub>2</sub> coating layers on the surface of GNPs strengthen the interfacial bonding, which results in that the stress be effectively transferred from the matrix to GNPs during loading. These findings indicate that the addition of GNPs can significantly enhance the mechanical properties of Al nanocomposites, while the TiO<sub>2</sub> particle layer coated on GNPs have a positive effect on this.

## **5 Declarations**

### **Availability of data and materials**

The datasets analyzed supporting the conclusions are included in this manuscript.

### **Competing interests**

The authors declare that they do not have competing financial interests or personal relationships that may affect the work reported in this manuscript.

### **Funding**

This research is supported by Technology Research Program of Jiangxi Provincial Department of Education for Higher School (GJJ190531).

#### **Authors' contributions**

Qingjie Wu designed the experiment. Zhenghua Guo, Wen He and Ning Li performed the experiment. Lihong Jiang and Guohui Tan processed experimental data and wrote this manuscript. All authors read and approved the final manuscript.

#### **Acknowledgments**

Not applicable.

#### **Authors' information**

Zheng-Hua Guo, born in 1972, is currently a professor at School of Aeronautic Manufacturing Engineering, Nanchang Hangkong University. His main research interests include the forming technology of alloys and the simulation plastic forming.

Qingjie Wu, born in 1985, is currently a PhD at School of Aeronautic Manufacturing Engineering, Nanchang Hangkong University. His research interests include the modification of Al-Mg alloys and the preparation of nonferrous metal composites.

Ning Li, born in 1980, is currently a PhD at School of Aeronautic Manufacturing Engineering, Nanchang Hangkong University. His main research is the modification of Al-Mg alloys. Li-Hong Jiang, born in 1983, is currently a PhD at

School of Aeronautic Manufacturing Engineering, Nanchang Hangkong University.

Her main research is the forming technology of alloy. Wen He, born in 1984, is currently a PhD at Analysis and Testing Center, Nanchang Hangkong University. He

mainly studies the microstructure optimization of alloys. Guo-Hui Tan, born in 1985, is currently a materials engineer in Jiangxi Jiangling Special Vehicle Co., Ltd., China.

## References

- [1] L.Y. Chen, Konishi, A. Fehrenbacher, M. Chao, J.Q. Xu, H. Choi, H.F. Xu, F.E. Pfeifferkorn & X.C. Li. (2012). Novel nanoprocessing route for bulk graphene nanoplatelets reinforced metal matrix nanocomposites. *Scripta Materialia*, 67(1), 29-32.
- [2] Andy Nieto, Ankita Bisht, Debrupa Lahiri, Z. Cheng & Arivind Agarwal. (2016). Graphene reinforced metal and ceramic matrix composites: a review. *Metallurgical Reviews*, 62(5), 241-302.
- [3] K.S. Novoselov. (2004). Electric field effect in atomically thin carbon films. *Science*, 306(5696), 666–669.
- [4] Z. Hu, G. Tong, D. Lin, C. Chen, H. Guo, J. Xu & L. Zhou. (2016). Graphene reinforced metal matrix nanocomposites-a review. *Materials Science and Technology*, 32(9), 903-953.
- [5] M. Shen, T. Chang, Hsieh, Y. Li, C. Chiang, H. Yang & M, Yip. (2013). Mechanical Properties and Tensile Fatigue of Graphene Nanoplatelets Reinforced Polymer Nanocomposites. *Journal of Nanomaterials*, 2013, 1-9.
- [6] D. Verma, P.C. Gope, A. Shandilya & A. Gupta. (2014). Mechanical-Thermal-Electrical and Morphological Properties of Graphene Reinforced Polymer Composites: A Review. *Transactions of the Indian Institute of Metals*, 67(6), 803-816.
- [7] X.H. Chen & H. Yan. (2015). Fabrication of nanosized Al<sub>2</sub>O<sub>3</sub> reinforced aluminum matrix composites by subtype multifrequency ultrasonic vibration.

*Journal of Materials Research*, 30(14), 2197-2209.

- [8] G. Li & B. Xiong. (2017). Effects of graphene content on microstructures and tensile property of graphene-nanosheets/aluminum composites. *Journal of Alloys and Compounds*, 697, 31-36.
- [9] H.P. Zhang, C. Xu, W.L. Xiao, K. Ameyama & C.L. Ma. (2016). Enhanced mechanical properties of Al5083 alloy with graphene nanoplates prepared by ball milling and hot extrusion. *Materials Science and Engineering: A*, 658, 8-15.
- [10] J. Wang, Z. Li, G. Fan, H. Pan, Z. Chen & D. Zhang. (2012). Reinforcement with graphene nanosheets in aluminum matrix composites. *Scripta Materialia*, 66(8), 594-597.
- [11] K.P. So, I.H. Lee, D.L. Duong, T.H. Kim, S.C. Lim, K.H. An. & Y.H. Lee. (2011). Improving the wettability of aluminum on carbon nanotubes. *Acta Materialia*, 59 (9), 3313-3320.
- [12] Y. Park, K. Cho, I. Park & Y. Park. (2011). Fabrication and mechanical properties of magnesium matrix composite reinforced with Si coated carbon nanotubes. *Procedia Engineering*, 10, 1446-1450.
- [13] S.I. Oh, J.Y. Lim, Y.C. Kim, J. Yoon, G.H. Kim, J. Lee, Y.M. Sung & J.H. Han. (2012). Fabrication of carbon nanofiber reinforced aluminum alloy nanocomposites by a liquid process. *Journal of Alloys and Compounds*, 542, 111-117.
- [14] A. Moya, A. Cherevan, S. Marchesan, P. Gebhardt, M. Prato, D. Eder & J.J. Vilatel. (2015). Oxygen vacancies and interfaces enhancing photocatalytic

- hydrogen production in mesoporous CNT/TiO<sub>2</sub> hybrids. *Applied Catalysis B Environmental*, 179(179), 574-582.
- [15] Q.H. Yuan, Z.Q. Qiu, G.H. Zhou, X.S. Zeng & Y. Liu. (2018). Interfacial design and strengthening mechanisms of AZ91 alloy reinforced with in-situ reduced graphene oxide. *Materials Characterization*, 138, 215-228.
- [16] Shao, P. & Zhen, Yang. (2018). Microstructure and tensile properties of 5083 Al matrix composites reinforced with graphene oxide and graphene nanoplates prepared by pressure infiltration method. *Composites Part A: Applied Science & Manufacturing*, 109, 151-162.
- [17] Wu, R. Wu, L. Hou, J. Zhang & M. Zhang. (2018). Microstructure, mechanical properties and wear performance of AZ31 matrix composites reinforced by graphene nanoplatelets (GNPs). *Journal of Alloys and Compounds*, 750(13), 530-536.
- [18] Yan H & H. Qiu. (2016). Fabrication of carbon nanotube reinforced A356 nanocomposites. *Journal of Materials Research*, 31(15), 2277-2283.
- [19] S.C. Cho, I. Jo, B.M. Jung, E. Lee, J.R. Choi, S.K. Lee & S.B. Lee. (2017). Interfacial analysis of TiO<sub>2</sub> coated carbon nanofibers and Mg-Al alloy matrix fabricated using a liquid pressing process. *Scripta Materialia*, 136, 50-54.
- [20] I. Jo, S.C. Cho, H. Kim, B.M. Jung, S.K. Lee & S.B. Lee. (2016). Titanium dioxide coated carbon nanofibers as a promising reinforcement in aluminum matrix composites fabricated by liquid pressing process. *Scripta Materialia*, 112, 87-91.

- [21]A. Bisht, M. Srivastava, R.M. Kumar, I. Lahiri & D. Lahiri. (2017). Strengthening mechanism in graphene nanoplatelets reinforced aluminum composite fabricated through spark plasma sintering. *Materials Science and Engineering*, 695, 20-28.
- [22]M. Rashad M, F. Pan, M. Asif & A. Tang. (2014). Powder metallurgy of Mg-1%Al-1%Sn alloy reinforced with low content of graphene nanoplatelets (GNPs). *Journal of Industrial and Engineering Chemistry*, 20(6), 4250-4255.
- [23]M. Rashad M, F. Pan, M. Asif & A. Tang. (2015). Improved strength and ductility of magnesium with addition of aluminum and graphene nanoplatelets (Al+GNPs) using semi powder metallurgy method. *Journal of Industrial and Engineering Chemistry*, 23, 243-250.

# Figures

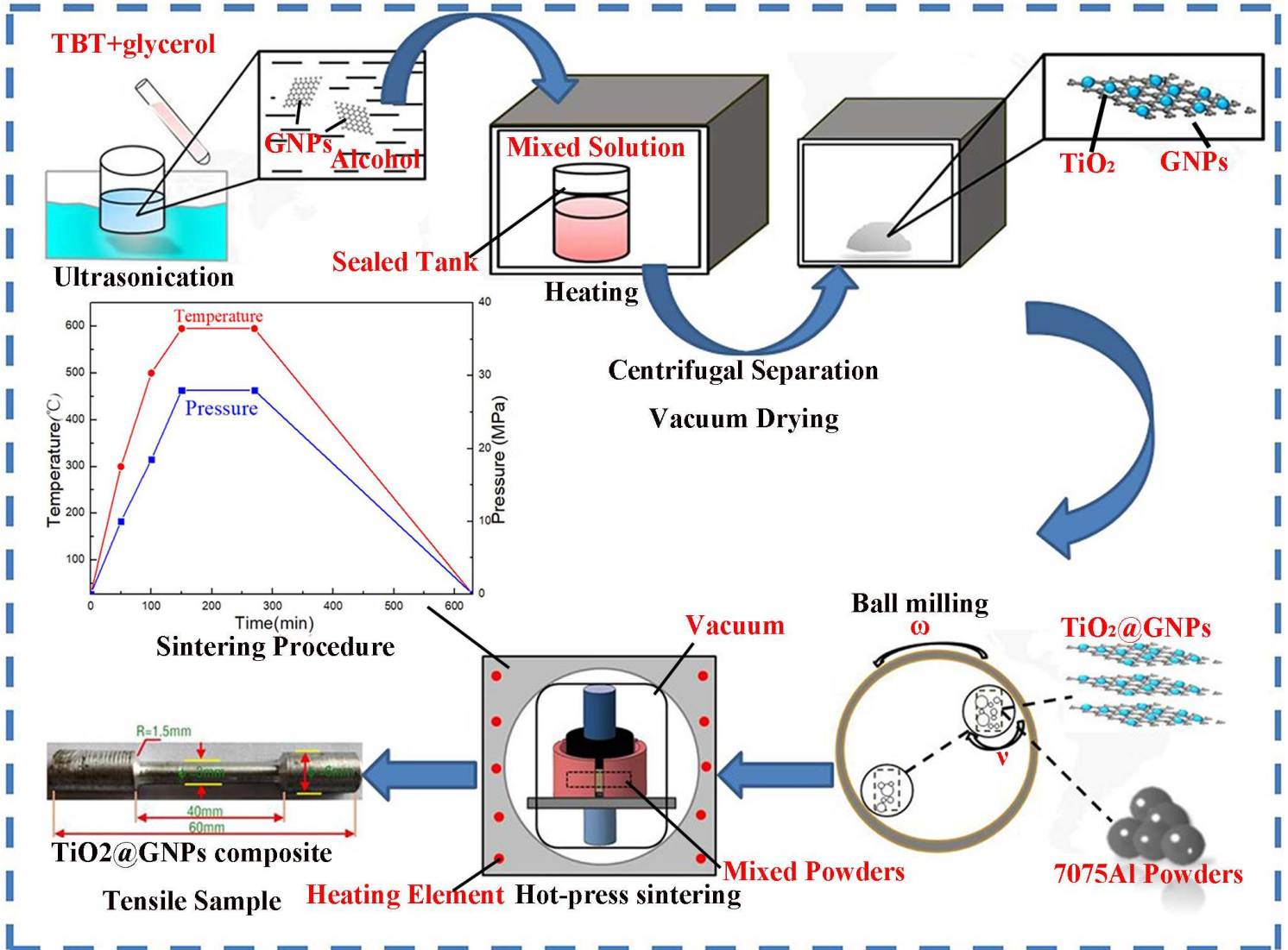
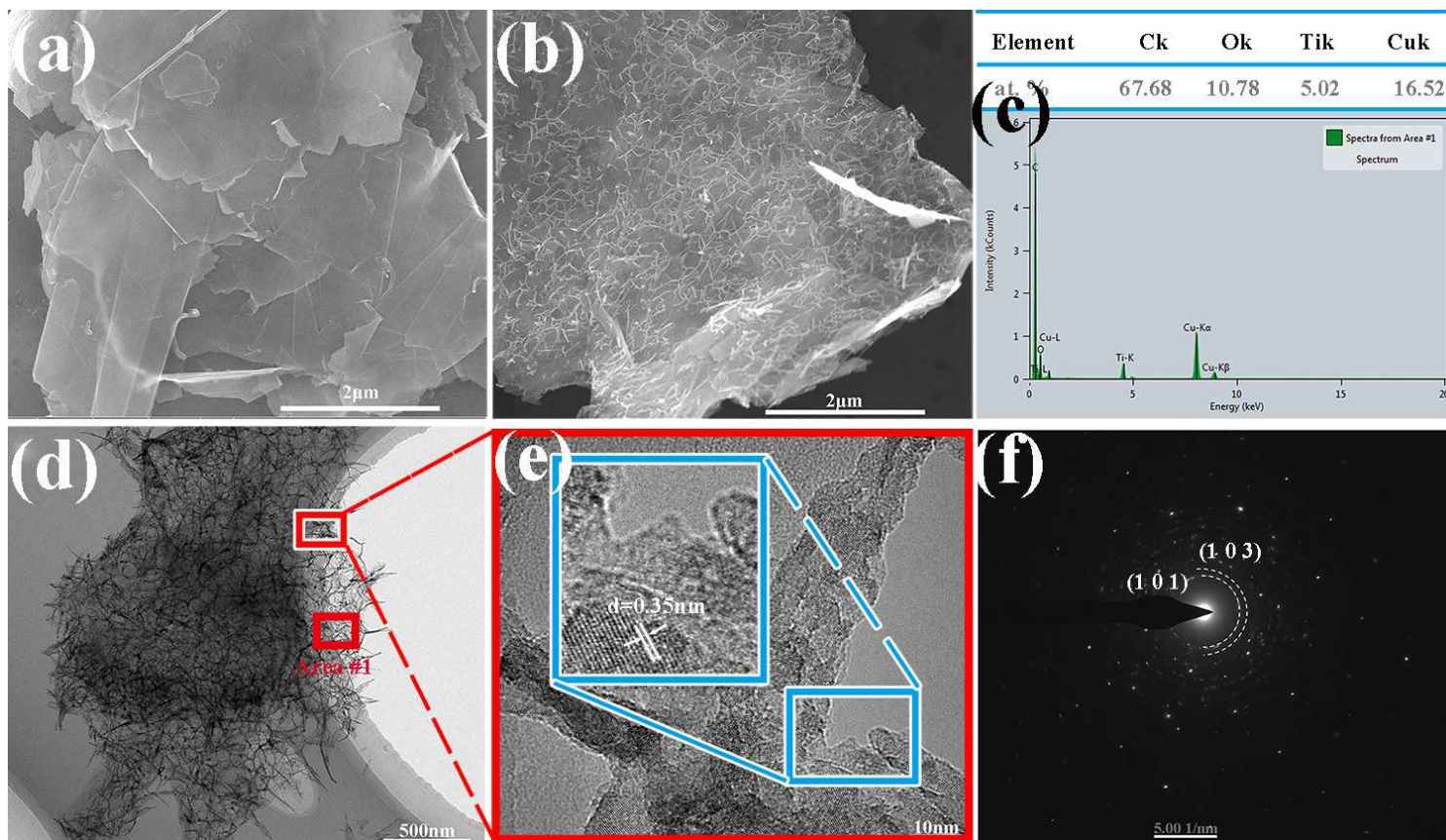


Figure 1

Schematic of the preparation of TiO<sub>2</sub>@GNPs / 7075Al nanocomposites.



**Figure 2**

SEM and TEM images of TiO<sub>2</sub>@GNPs: (a) SEM image of GNPs. (b) SEM image of TiO<sub>2</sub>@GNPs. (c) EDX results of Area#1. (d) TEM image of TiO<sub>2</sub>@GNPs. (e) HRTEM image of TiO<sub>2</sub>@GNPs. (f) SAED patterns of TiO<sub>2</sub> layer.

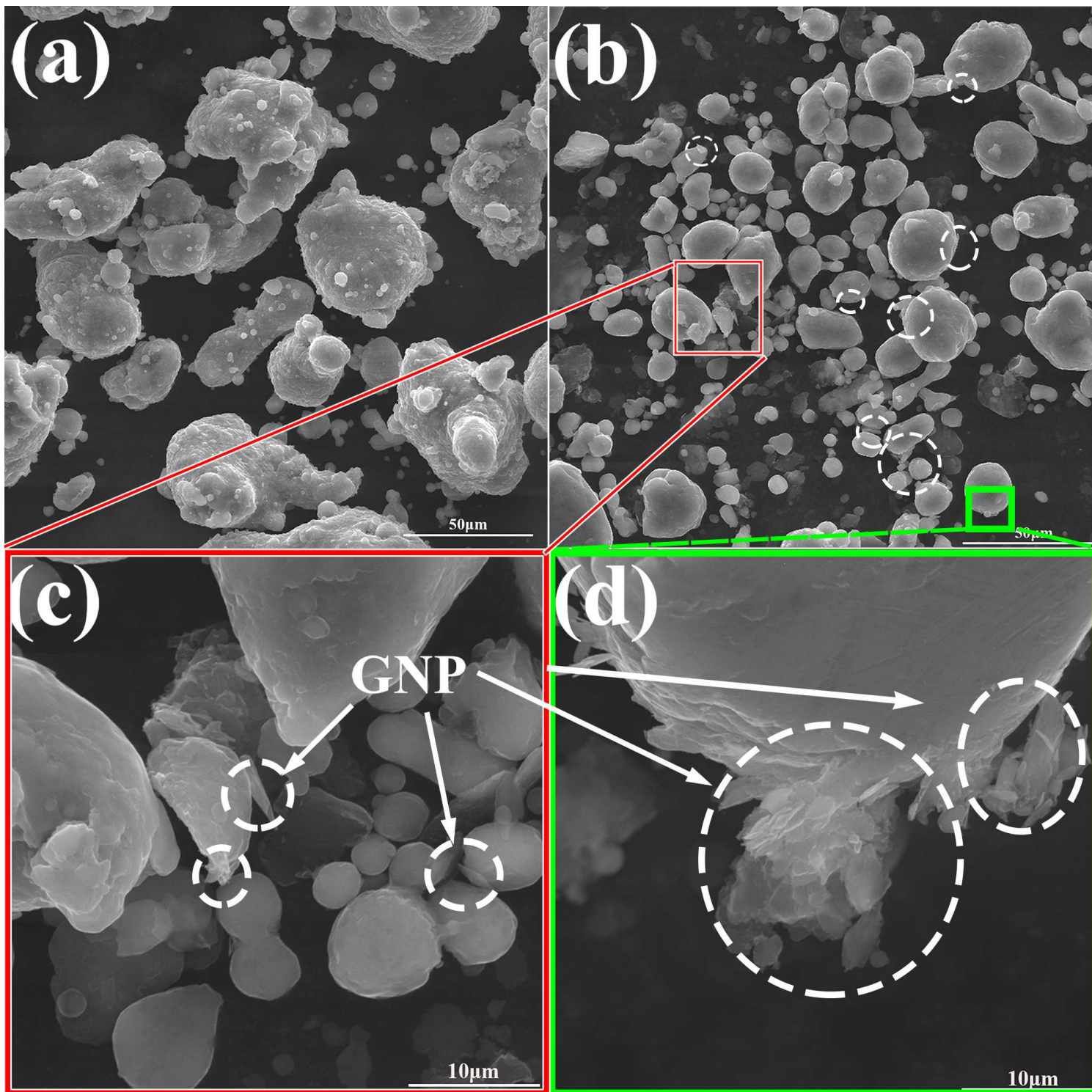


Figure 3

Micrographs of composite precursor powders

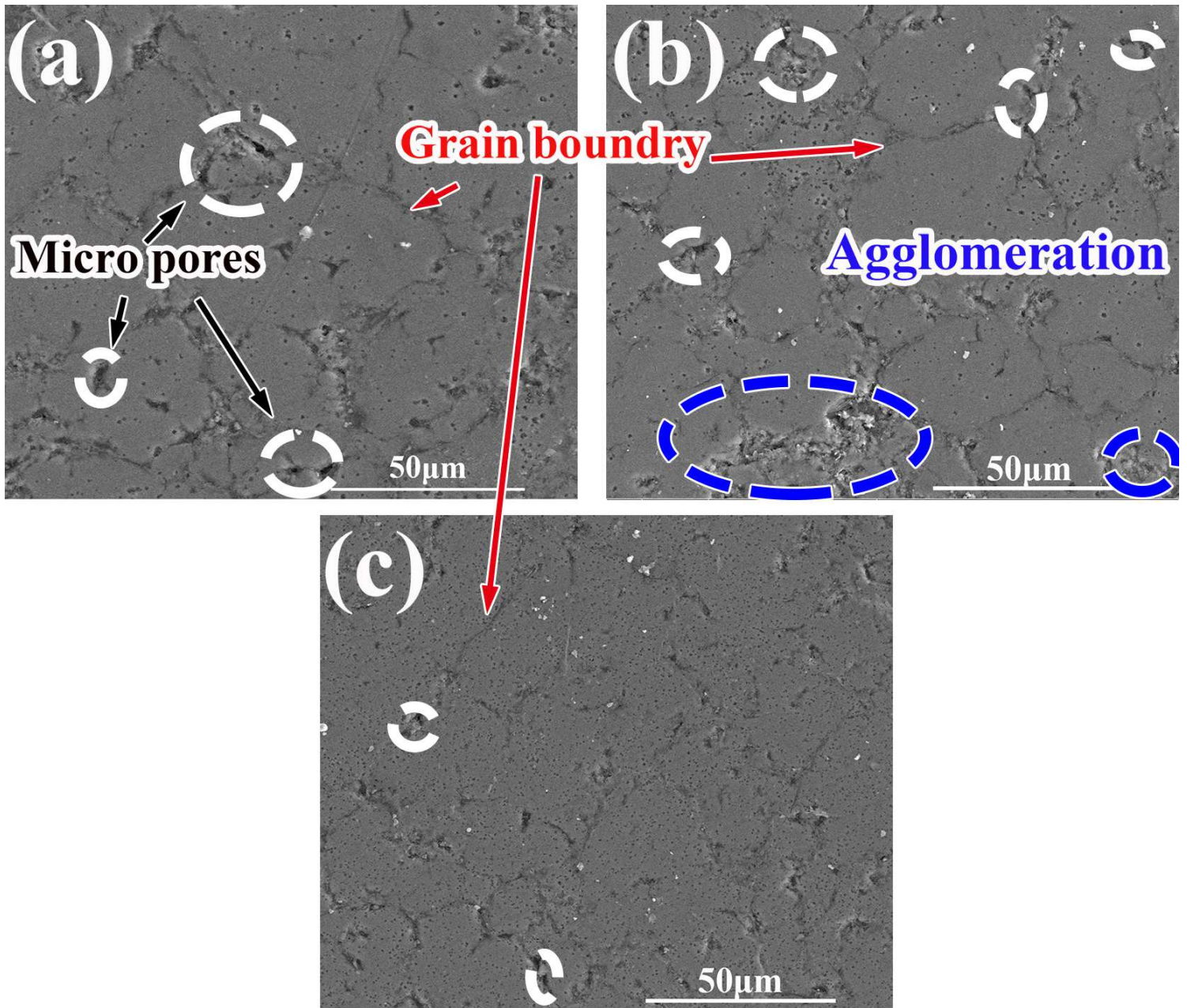


Figure 4

Micrographs of 7075Al and corresponding nanocomposites: (a) 7075Al, (b) GNPs/7075Al, (c) TiO<sub>2</sub>@GNPs/7075Al

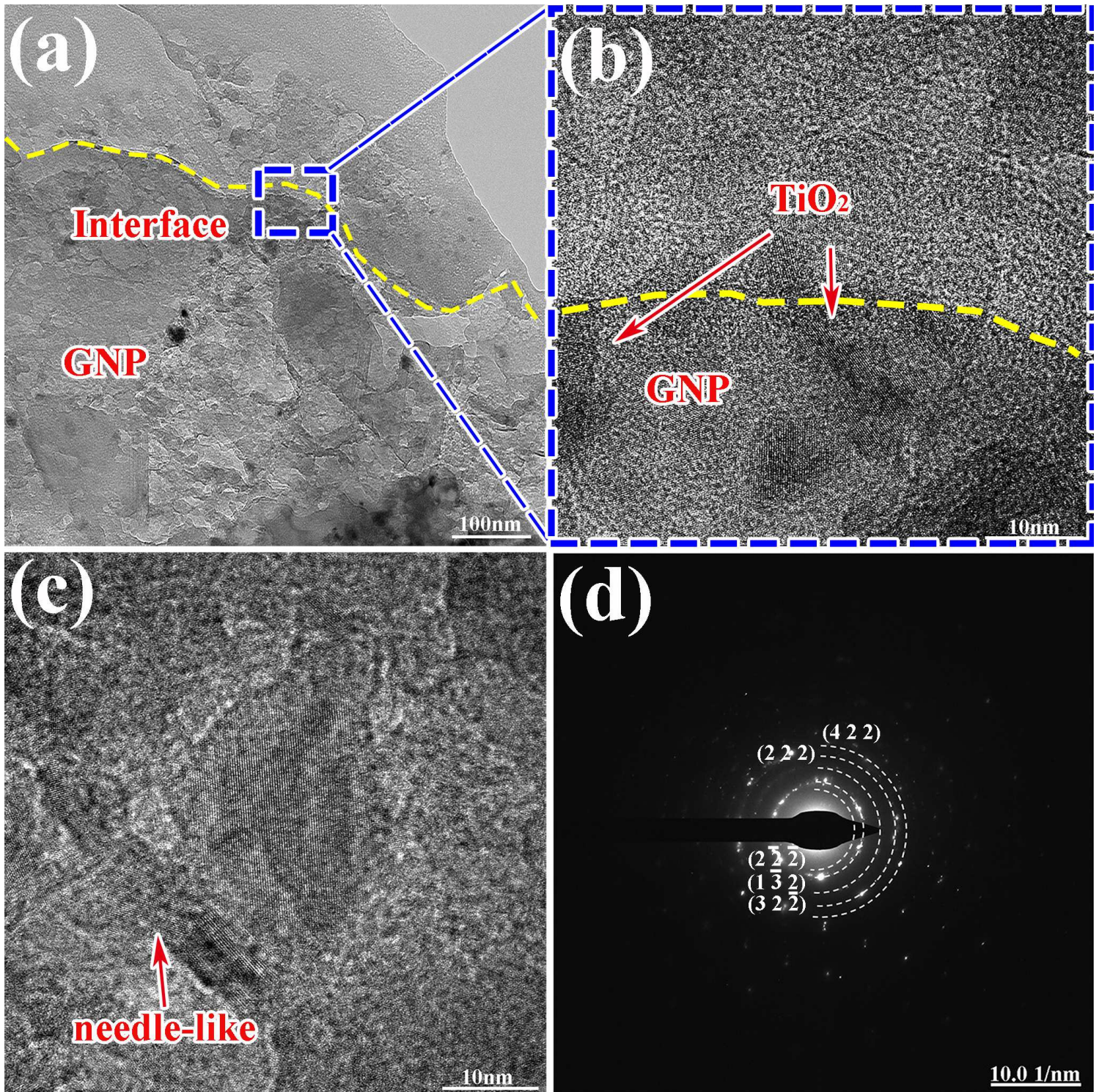
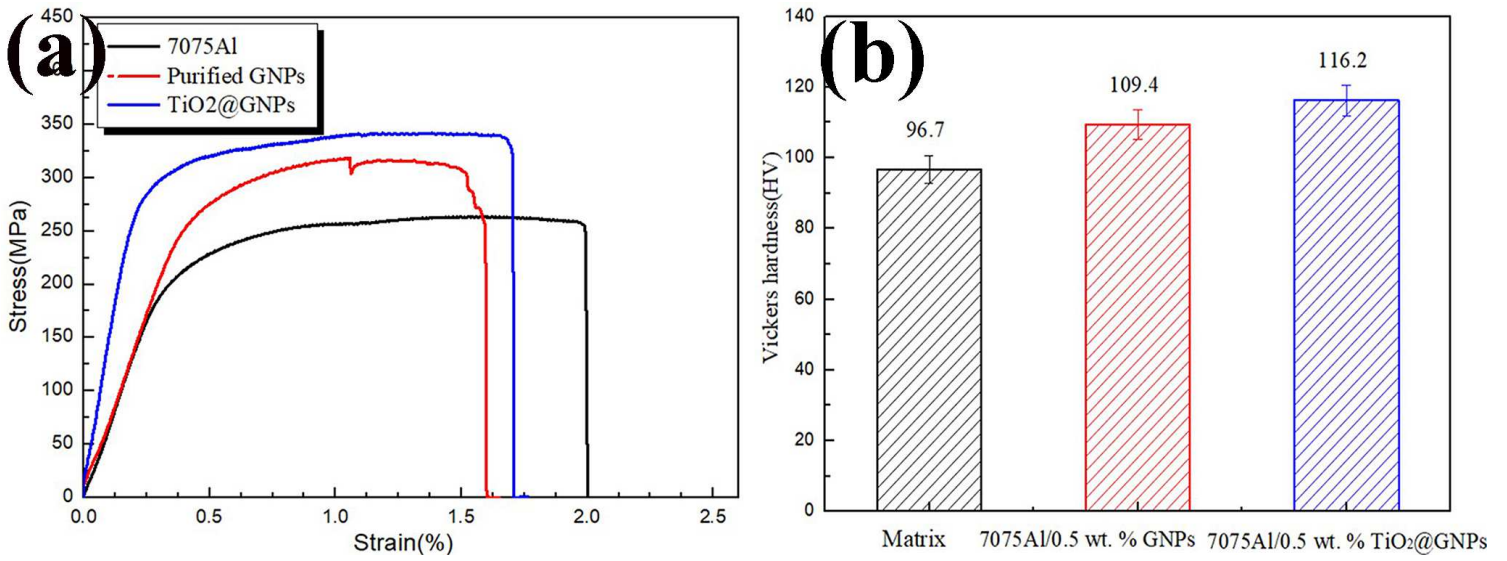


Figure 5

TEM images of (a), (b) and (c) TiO<sub>2</sub>@GNPs/7075Al nanocomposites fabricated, (d) SAED patterns of coating layer.



**Figure 6**

Mechanical behaviors of 7075Al matrix and its nanocomposites reinforced with purified GNPs or TiO<sub>2</sub>@GNPs